

PAPER • OPEN ACCESS

Numerical Simulation Study on Electromagnetic Force Constrained Liquid Metal Deformation

To cite this article: Huaxiang Zhang and Bin Lei 2019 *IOP Conf. Ser.: Mater. Sci. Eng.* **493** 012102

View the [article online](#) for updates and enhancements.

You may also like

- [Numerical analysis on the effect of process parameters on deposition geometry in wire arc additive manufacturing](#)
Shilong FAN, , Fei YANG et al.
- [Numerical analysis of the pre-arcing liquid metal self-pinch effect for current-limiting applications](#)
Yiyi Liu, Mingzhe Rong, Yi Wu et al.
- [Experimental study on liquid metal free surface flow under magnetic and electric field for nuclear fusion](#)
Xu Meng, Zenghui Wang and Dengke Zhang

ECS
The
Electrochemical
Society
Advancing solid state &
electrochemical science & technology

DISCOVER
how sustainability
intersects with
electrochemistry & solid
state science research

Numerical Simulation Study on Electromagnetic Force Constrained Liquid Metal Deformation

Huaxiang Zhang ^a, Bin Lei ^b

Shijiazhuang Campus, Army Engineering University, Shijiazhuang 050003, China.

^aZhanghx0129@126.com, ^b13014370266@163.com

Abstract. In order to explore the mechanism of electromagnetic force restraining the deformation of liquid metal with non-uniform diameter, the coupling simulation of electromagnetic field and flow field was carried out to study the distribution of electromagnetic field and flow field in liquid metal. The simulation results show that the electromagnetic force at the convex position of the liquid metal is the largest, while the electromagnetic force at the concave position is smaller, and the diameter of the liquid metal with non-uniform diameter tends to be the same under the action of the pressure difference of the electromagnetic force.

Keywords: liquid metal, magnetic force, constraint, deformation.

1. Introduction

Researchers have found that the penetration power of metal jets is proportional to the effective length through a large number of theoretical calculations and numerical simulations[1-3]. When the metal jets fly under electromagnetic field, the development of necking state can be delayed, the effective length can be extended, and the penetration depth of metal jets can be enhanced. Because the measurement of the length and shape of metal jet under the action of electromagnetic field involves some difficult problems such as the explosion of armor-piercing projectile and the timing control of the application of intense pulsed magnetic field[4], the measurement is difficult and dangerous. There is lack of experimental data to verify and improve the theoretical and simulation results. Only part of the research compares the electromagnetic field. The change of penetration ability of metal jet after action indirectly shows that the effective length of metal jet is increased under the action of electromagnetic field.

Because the physical properties of liquid metal and metal jet are similar, it is convenient to measure the morphological changes of liquid metal under electromagnetic field, which can lay a foundation for measuring the effective length changes of metal jet under electromagnetic field. In order to measure the deformation of liquid metal before the experiment, the distribution law of electromagnetic field and flow field in liquid metal under the action of electromagnetic field was simulated, and the variation law of magnetic induction intensity, induced current density, electromagnetic force density and deformation velocity with time was analyzed. The simulation results were preliminarily verified. The effective length of metal jets increases under the action of electromagnetic field.



2. Simulation model establishment and parameter setting

Induction heat has little effect on the viscosity and deformation of liquid metal, so it ignores its effect. Because of the rotational symmetry of the model, a two-dimensional model is used to simulate the model. As shown in Figure 1, the diameter of the liquid metal simulation model is 3mm-8mm, and the contour is changed according to the cosine function $r=1.25*\cos(2*\pi/5*z)+2.75$, in which r is the radius, z is the axial length and the total length is 15mm; the two series coils are solenoid coils made of single-turn copper wire, each coil length is 155mm, the inner diameter is 31mm, the cross-section of copper wire is 2mm×4mm rectangular, the line The number of turns is 31 turns, and the two coils are 15.5mm, which is exactly equal to the radius of the coil. The resistance and inductance values of two series coils are calculated according to the theoretical formula: $R=13.7m\Omega$ and $L=12.2\mu H$. The excitation loading circuit is shown in Figure 2, the capacitor capacitance is $C=250\mu F$, and the charging voltage is $U=7000V$.

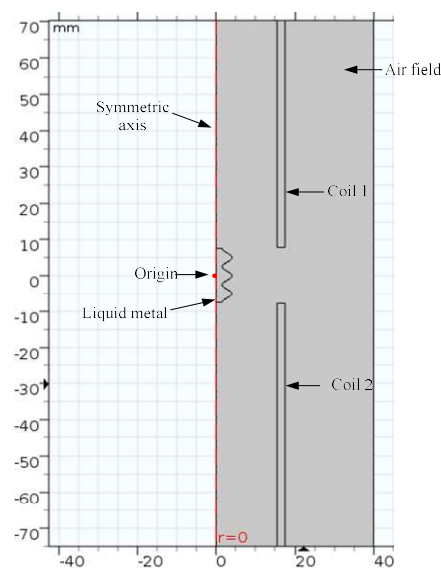


Fig.1 Simulation model of electromagnetic field constraint

The following assumptions are made in the calculation: (1) The liquid metal $Ga_{67}In_{20.5}Sn_{12.5}$ is an incompressible conductive fluid, and all physical parameters of the liquid metal such as density, viscosity, conductivity and permeability are scalar constants, and their physical properties are shown in Table 1; (2) The displacement current and the resistance of the conductor in the liquid metal are neglected, while the induction is neglected. The effect of electric current on the heating of liquid metal is that the viscosity of liquid metal does not change. (3) The influence of liquid metal flow on electromagnetic field is neglected. The applied current is in the positive direction, i.e. perpendicular to the paper face, and is considered to be evenly distributed across the wire section. Because the Reynolds number of liquid metal is small, the flow field is laminar. The liquid metal model grid is set as a moving grid to ensure the flow deformation of liquid metal under electromagnetic force. The computation time is $5 \times 10^{-4}s$ and the step length is $2 \times 10^{-6}s$.

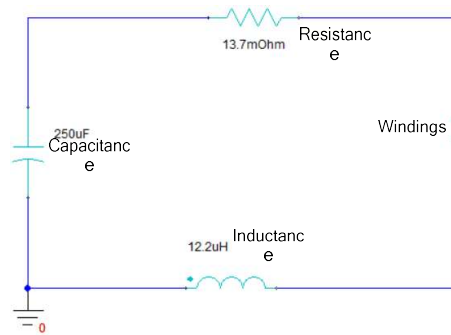


Fig.2 Excitation loading circuit

Table.1 Physical properties of Ga₆₇In_{20.5}Sn_{12.5}

Density/ $Kg \cdot m^{-3}$	Specific heat/ $J \cdot Kg^{-1} \cdot K^{-1}$	Electric conductivity $/ S \cdot m^{-1}$	Thermal conductivity/ $W \cdot m^{-1} \cdot K^{-1}$	Dynamic viscosity/ $Kg \cdot m^{-1} \cdot s^{-1}$	Relative permeability
6360	481	3.1×10^6	39	0.002162	1

3. Simulation results and analysis

3.1. Electromagnetic field analysis.

Fig. 3 is a nephogram of magnetic induction intensity distribution in the middle region of two solenoid coils at $t=8 \mu s$. It is found that the magnetic field intensity decreases sharply at the end of the solenoid coil and distributes gradually along the axial direction of the coil, that is, the magnetic induction intensity at point 1 is greater than the corresponding value at point 2 and point 3, while the magnetic induction intensity in liquid metal tends to skin. Because point 1 is closer to the end of the coil, the magnetic induction intensity at point 1 is always greater than the corresponding value at point 2 and point 3, but the magnetic induction intensity at the three points is not very different.

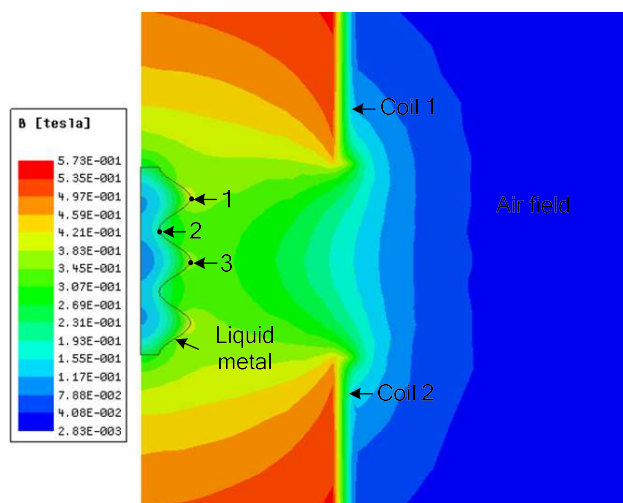


Fig.3 Distribution of magnetic flux density in the middle region of solenoid coil

Fig. 4 shows the variation of induced current density with time at midpoint 1, 2 and 3 in Fig. 3. The positive and negative values represent the direction of induced current density. The analysis shows that

when $t \leq 142 \mu s$, $280 \mu s \leq t \leq 426 \mu s$, the flux of induction current obstructs the increase of magnetic flux caused by coil current, and the direction of induction current density is opposite to solenoid coil current; when $142 \mu s \leq t \leq 280 \mu s$, $426 \mu s \leq t \leq 500 \mu s$, the solenoid coil current decreases and the excitation magnetic flux decreases. The flux of induction current impedes the decrease of the flux, so the direction of induction current density is the same as that of solenoid coil. The figure shows that the maximum induction current density of protrusion is $2.59 \times 10^8 A/m^2$, the maximum induction current density of depression is $9.26 \times 10^7 A/m^2$, and the variation trend of induction current of three positions is the same, and the protrusion (such as point 1, point 3) The induced current density is much higher than the corresponding value of the depression (e.g. point 2) because the protrusion is closer to the inner surface of the coil and the magnetic field coupling is stronger than the depression; the radial radius of point 1 and point 3 is the same, the axial position is different, and the induced current density is slightly different.

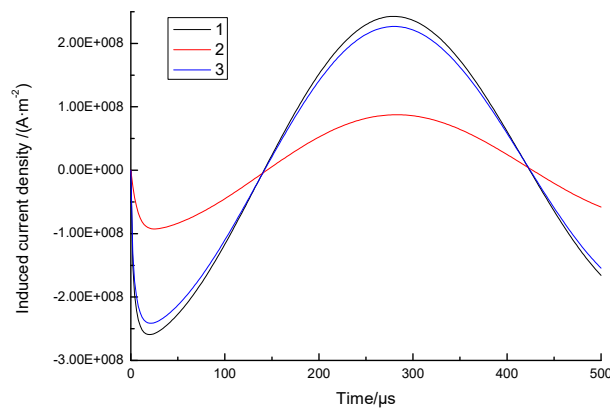


Fig.4 Curves of induced current density varying with time

Fig.5 shows the variation of electromagnetic force density with time. The magnitude of electromagnetic force density is determined by the product of induced current density and magnetic induction intensity, but the magnitude of induced current density is much larger than that of magnetic induction intensity. Therefore, the magnitude of electromagnetic force density is mainly determined by the induced current density, and the positive and negative magnitudes represent the pulling of liquid metal respectively. Force and pressure. The analysis shows that the electromagnetic force density is closely related to the position and coil current. The electromagnetic force at the bulge is obviously greater than the corresponding value at the depression. When the electromagnetic force is pressure, it will drive the liquid metal from the bulge to the depression, which is beneficial to reduce the diameter difference of the liquid metal. Under tensile stress, the resultant force of the axial and radial components of the electromagnetic force stretches along the arc surface of the liquid metal, driving the liquid metal in the bulge to flow to the depression, thus still conducive to reducing the diameter of the liquid metal.

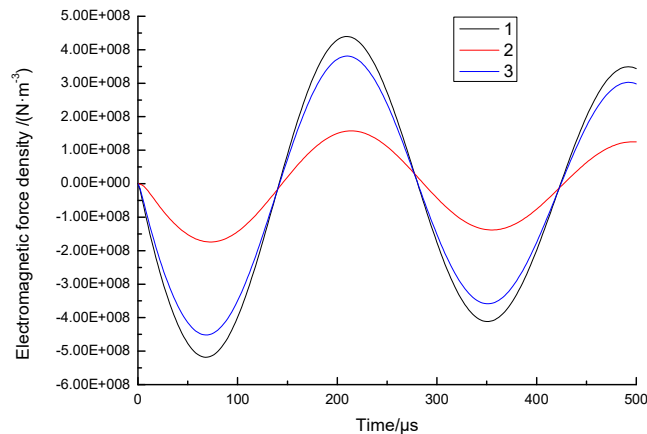


Fig.5 Variation of electromagnetic force density with time

3.2. Flow field analysis.

Fig. 6 shows the variation of deformation of liquid metal with time at the convex and concave points. Deformation refers to the increase or decrease of the diameter of liquid metal points 1 and 2 in Fig. 3. It can be found from the diagram that the deformation of the bulge is always greater than the corresponding value of the depression, because the diameter of the bulge is larger, and the effect of electromagnetic force is more obvious. When $t \leq 200 \mu\text{s}$, the deformation rate of the electromagnetic force bulge is the largest in the whole electrification process. When $200 \mu\text{s} \leq t \leq 320 \mu\text{s}$, the deformation of the bulge and the depression is small and the deformation rate is slow due to the change of the direction of the electromagnetic force. However, the change of the direction of the electromagnetic force in the depression lags behind the bulge due to the skin effect. The influence of electromagnetic force on the deformation is lagged behind the bulge. When $320 \mu\text{s} \leq t \leq 500 \mu\text{s}$, the electromagnetic force changes direction again, the diameter of the restraint bulge decreases, and the liquid metal flows and deforms from the bulge to the depression. Accordingly, the diameter of the depression increases. The ratio of the maximum diameter to the minimum diameter of the liquid metal is 2.67 before electrifying. After electrifying $500 \mu\text{s}$, the ratio of the maximum diameter to the minimum diameter is 1.76. The diameter of the liquid metal tends to be more uniform under the action of the electromagnetic field, and the reduction of the diameter of the liquid metal can be equivalent to the increase of the length, that is, the liquid metal with non-uniform diameter is in the electromagnetic field. According to the similarity of physical properties between liquid metal and metal jet, the conclusion that the diameter of metal jet under electromagnetic field tends to be consistent can be preliminarily verified.

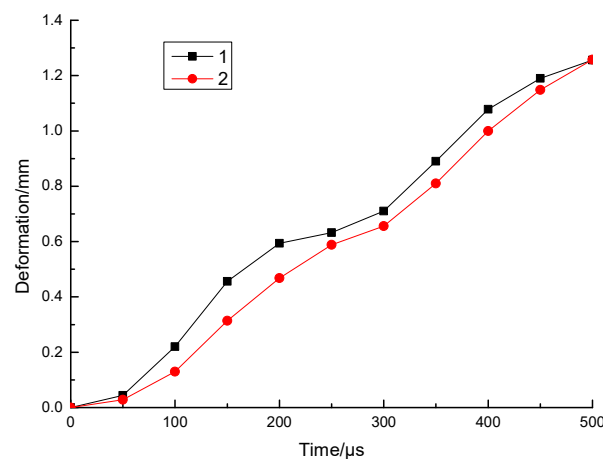


Fig.6 Variation of deformation with time

4. Conclusion

(1) After the coil is electrified, the magnetic induction intensity, the induced current density and the electromagnetic force density all have obvious skin effect. The value is closely related to the position and the coil current. The electromagnetic force density is mainly determined by the induced current density, and the electromagnetic force in the bulge is greater than that in the depression. Therefore, the liquid metal is in the electricity. Deformation occurs under magnetic force.

(2) Under the action of electromagnetic force, the diameter of the bulge decreases, the diameter of the depression increases, and the ratio of the maximum diameter to the minimum diameter of the liquid metal decreases from 2.67 to 1.76. The diameter of the liquid metal is obviously more uniform, which can preliminarily verify the conclusion that the diameter of the metal jet under the action of electromagnetic field tends to be consistent.

References

- [1] Fedorov S V, Babkin A V, Ladov S V, et al. Possibilities of controlling the shaped-charge effect by electromagnetic actions[J]. *Combustion, Explosion, and Shock Waves*, 2000, 36(6): 792-808.
- [2] Fedorov S V. Magnetic stabilization of elongation of metal shaped charge jets[C]//*Proc. 25th Int. Symp.* Beijing, China: Science and Technology Press, 2010: 967-975.
- [3] Shvetsov G A, Matrosov A D, Stankevich S V. Effect of electric current on the depth of penetration of shaped-charge jets into targets[J]. *Journal of Applied Mechanics and Technical Physics*, 2015, 56(1): 125-135.
- [4] Ma B, Huang Z, Xiao Q, et al. Effect of External Magnetic Field Loaded at the Initial Period of Inertial Stretching Stage on the Stability of Shaped Charge Jet[J]. *IEEE Transactions on Plasma Science*, 2017, 45(5): 875-881.